

**Supporting Information for**

**A machine learning-assisted study of the formation of oxygen  
vacancies in anatase titanium dioxide**

Dan Wang,<sup>+,a</sup> Ronghua Zan,<sup>+,b</sup> Xiaorong Zhu,<sup>\*,c</sup> Yuwei Zhang,<sup>a</sup> Yu Wang,<sup>a</sup> Yanhui Gu,<sup>\*,b</sup> and Yafei Li<sup>\*,a</sup>

<sup>a</sup>Jiangsu Key Laboratory of New Power Batteries, Jiangsu Collaborative Innovation Centre of Biomedical Functional Materials, School of Chemistry and Materials Science, Nanjing Normal University, Nanjing, 210023, P. R. China

<sup>b</sup>School of Computer Science and Technology, Nanjing Normal University, Nanjing 210023, P. R. China

<sup>c</sup>College of Chemistry and Chemical Engineering, Nantong University, Nantong 226019, P. R. China

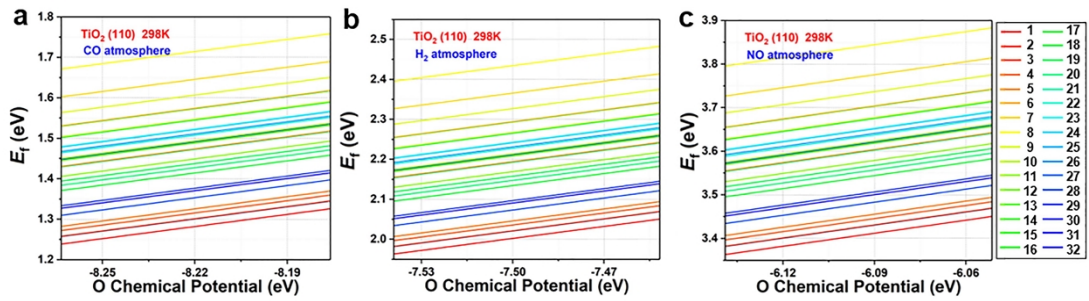


**Figure S1.** The O vacancy formation energy of the uppermost layer of O atoms on  $\text{TiO}_2$ (110), under CO, H<sub>2</sub> and NO atmosphere when set the reaction temperature to be 298 K.

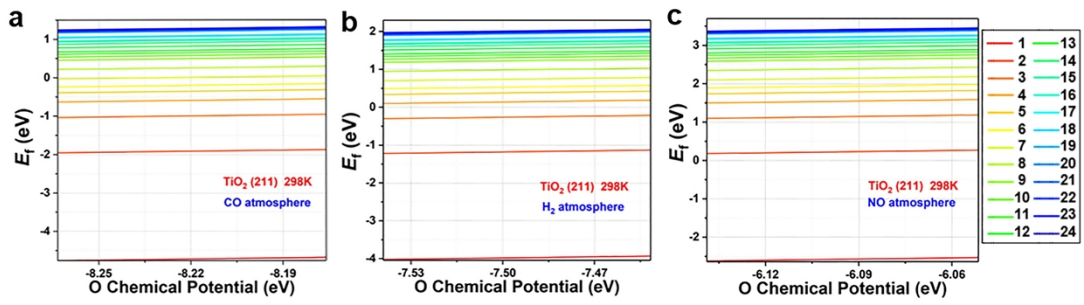


**Figure S2.** The O vacancy formation energy of the uppermost layer of O atoms on  $\text{TiO}_2$  (211), under CO, H<sub>2</sub> and NO atmosphere when set the reaction temperature to be 298 K.

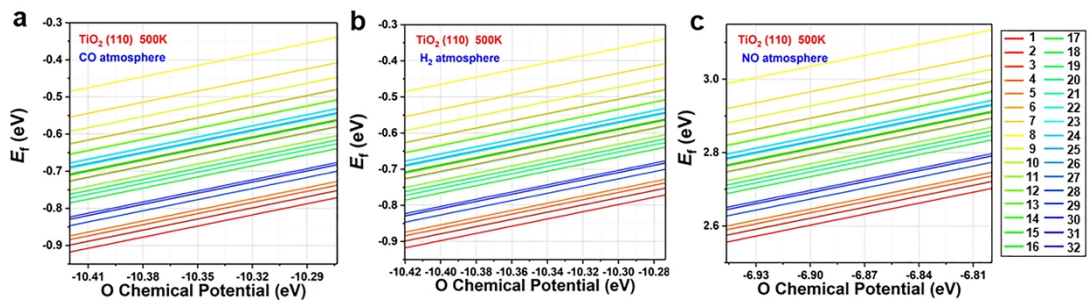


**Figure S3.** The O vacancy formation energy of the uppermost layer of O atoms on  $\text{TiO}_2$  (110), under CO,  $\text{H}_2$  and NO atmosphere when set the reaction temperature to be 500 K.

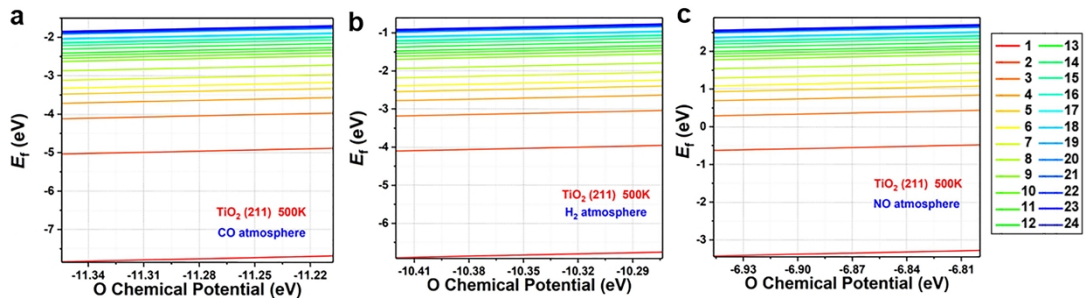


**Figure S4.** The O vacancy formation energy of the uppermost layer of O atoms on  $\text{TiO}_2$  (211), under CO, H<sub>2</sub> and NO atmosphere when set the reaction temperature to be 500 K.

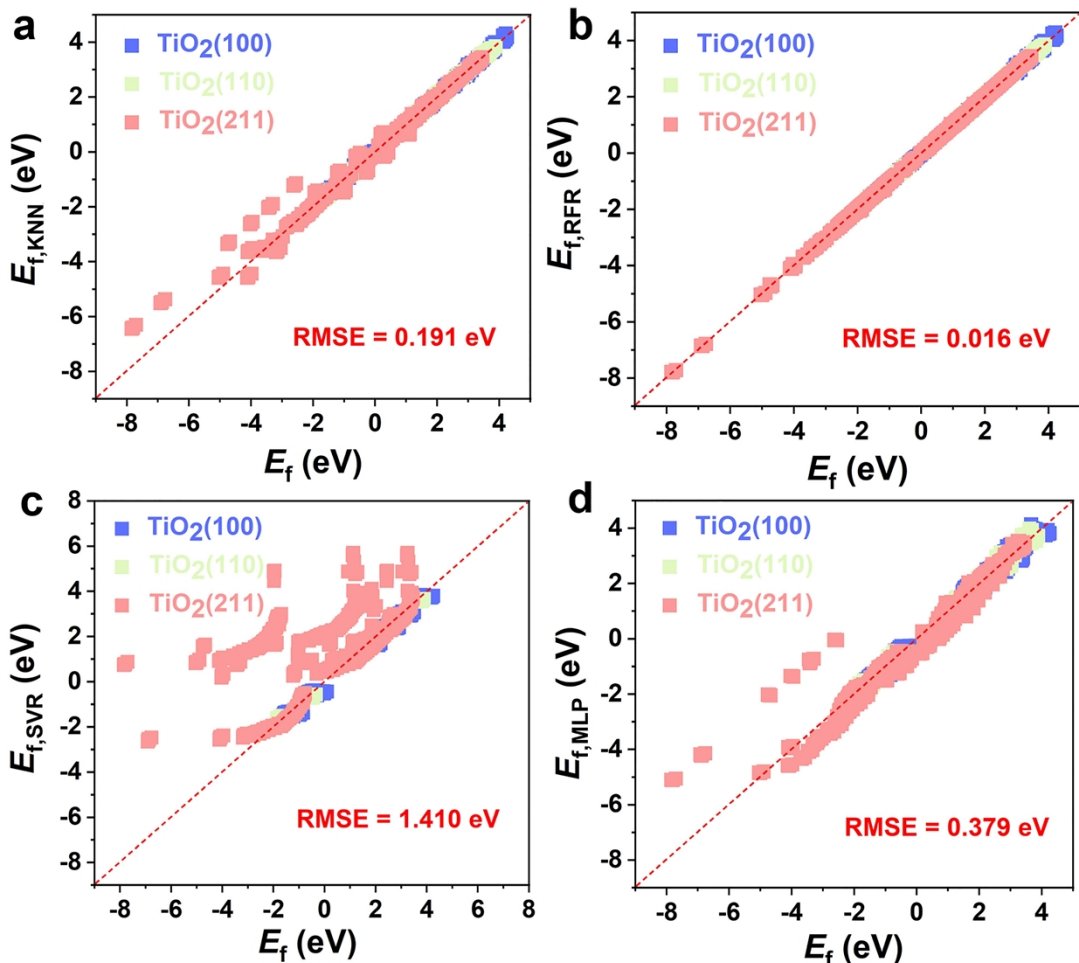


**Figure S5.** The comparison between DFT calculated  $E_f$  and (a)KNN, (b) RFR, (c)SVR, (d)MLP predicted values on  $\text{TiO}_2(100)$ ,  $\text{TiO}_2(110)$ ,  $\text{TiO}_2(211)$ .

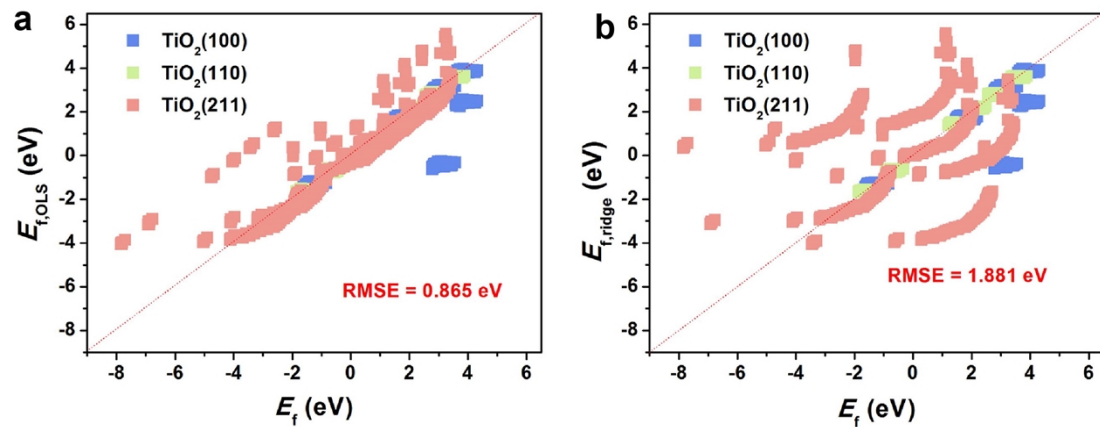


**Figure S6.** The compassion between DFT calculated  $E_f$  and (a)OLS, (b)ridge predicted values on  $\text{TiO}_2(100)$ ,  $\text{TiO}_2(110)$ ,  $\text{TiO}_2(211)$ .

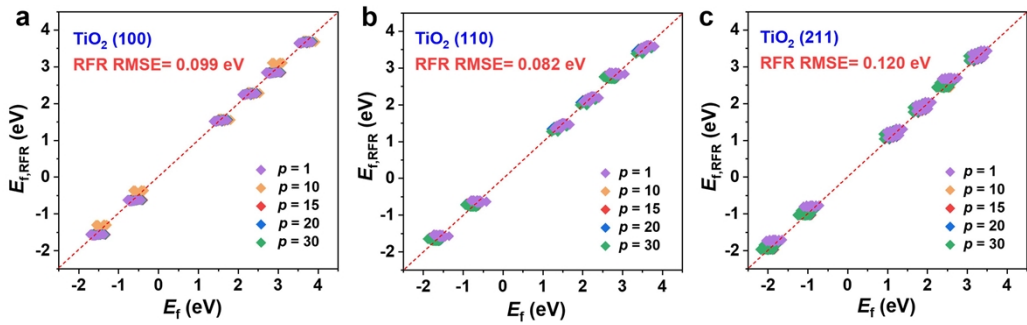


**Figure S7.** Comparison between the  $E_f$  of the second O layer predicted by the ML based on the RFR model and the results calculated by DFT for (a)  $\text{TiO}_2$ (211), (b)  $\text{TiO}_2$ (110), and (c)  $\text{TiO}_2$ (100) surfaces. The purple, yellow, red, blue, and green dots represent the partial pressure ratio of 1, 10, 15, 20, and 30, respectively.

**Table S1.** The SISSO algorithm uses different numbers of features to construct equations for  $E_f$ .

| Features                                    | Equation  | RMSE      |
|---|---|-----------|
| $n, p, T, \gamma,$<br>$\mu_1, \mu_2, \mu_3$ | $E_f = (0.943(p + n) - 0.640(p \times \gamma))\left(\frac{\mu_3}{n}\right) - 0.301\frac{p \times \mu_3}{n \times \gamma} + 9.154$ | 0.7106 eV |
| $n, T, \gamma,$<br>$\mu_1, \mu_2, \mu_3$    | $E_f = \left(2.973\mu_3 - 2.049(\mu_3 \times \gamma) - 3.164\frac{\gamma}{n}\right)\gamma + 9.356$                                | 0.7112 eV |
| $n, T, \gamma,$<br>$\mu_2, \mu_3$           | $E_f = \left(2.973\mu_3 - 2.049(\mu_3 \times \gamma) - 3.164\frac{\gamma}{n}\right)\gamma + 9.356$                                | 0.7112 eV |
| $n, \gamma, \mu_2,$<br>$\mu_3$              | $E_f = \left(2.973\mu_3 - 2.049(\mu_3 \times \gamma) - 3.164\frac{\gamma}{n}\right)\gamma + 9.356$                                | 0.7112 eV |
| $\gamma, \mu_2, \mu_3$                      | $E_f = (0.035\mu_3 + 4.024 - 2.525\gamma)(\mu_3 \times \gamma) + 11.367$  | 0.8003 eV |
| $\gamma, \mu_3$                             | $E_f = 7.832\mu_3 + 2597.384\frac{1}{\mu_3} + 8401.311\frac{1}{\mu_3^2} + 254.794$  | 1.0002 eV |